Absence of COVID-19-associated changes in plasma coagulation proteins and pulmonary thrombosis in the ferret model

Iris C. Kreft [a], Roy R.A. Winiarczyk [b,c], Fric J. Tanis [b,c], Carmen van der Zwaan [a], Katharina S. Schmitz [d], Arie J. Hoogendijk [a], Rik L. de Swart [d], Anne Moscona [e], Matteo Porotto [e], Daniela C.F. Salvatori [f,g], Rory D. de Vries [d], Moniek P.M. de Maat [h], Maartje van den Biggelaar [a], Bart J.M. van Vlijmen [b,c,*], Dutch Covid-19 and Thrombosis Coalition (DCTC)

[a] Department of Molecular Hematology, Sanquin Research, Amsterdam, the Netherlands
[b] Einthoven Laboratory for Vascular and Regenerative Medicine, Leiden University Medical Center, Leiden, the Netherlands
[c] Department of Internal Medicine, Division of Thrombosis and Hemostasis, Leiden University Medical Center, Leiden, the Netherlands
[d] Department Viroscience, Erasmus MC, Rotterdam, the Netherlands
[e] Department of Pediatrics, Columbia University Vagelos College of Physicians and Surgeons, New York, NY, USA
[f] Central Laboratory Animal Facility, Leiden University Medical Center, Leiden, the Netherlands
[g] Anatomy and Physiology, Clinical Sciences, Faculty of Veterinary Medicine, Utrecht University, Utrecht, the Netherlands
[h] Department of Hematology, Erasmus MC, Erasmus University Medical Center, Rotterdam, the Netherlands

A R T I C L E   I N F O

S U M M A R Y

Background: Many patients who are diagnosed with coronavirus disease 2019 (COVID-19) suffer from venous thromboembolic complications despite the use of stringent anticoagulant prophylaxis. Studies on the exact mechanism(s) underlying thrombosis in COVID-19 are limited as animal models commonly used to study venous thrombosis pathophysiology (*i.e.* rats and mice) are naturally not susceptible to Severe Acute Respiratory Syndrome Coronavirus 2 (SARS-CoV-2). Ferrets are susceptible to SARS-CoV-2 infection, successfully used to study virus transmission, and have been previously used to study activation of coagulation and thrombosis during influenza virus infection.
Objectives: This study aimed to explore the use of (heat-inactivated) plasma and lung material from SARS-CoV-2-inoculated ferrets studying COVID-19-associated changes in coagulation and thrombosis.
Material and methods: Histology and longitudinal plasma profiling using mass spectrometry-based proteomics approach was performed.
Results: Lungs of ferrets inoculated intranasally with SARS-CoV-2 demonstrated alveolar septa that were mildly expanded by macrophages, and diffuse interstitial histiocytic pneumonia. However, no macroscopical or microscopical evidence of vascular thrombosis in the lungs of SARS-CoV-2-inoculated ferrets was found. Longitudinal plasma profiling revealed minor differences in plasma protein profiles in SARS-CoV-2-inoculated ferrets up to 2 weeks post-infection. The majority of plasma coagulation factors were stable and demonstrated a low coefficient of variation.
Conclusions: We conclude that while ferrets are an essential and well-suited animal model to study SARS-CoV-2 transmission, their use to study SARS-CoV-2-related changes relevant to thrombotic disease is limited.

1. Introduction

Many patients who are diagnosed with COVID-19 suffer from Severe Acute Respiratory Syndrome Coronavirus 2 (SARS-CoV-2)-induced thrombo(embolic) complications. Klok et al. [1] studied the incidence of

venous thromboembolisms (VTE) among COVID-19 patients in intensive care units (ICU), showing that despite daily administration of anticoagulants, over 30% of these COVID-19 patients developed thrombo(embolic) complications. This was significantly higher compared to non-COVID ICU patients, indicating that SARS-CoV-2 may induce a strong

pro-thrombotic trigger [2]. Furthermore, when studying the therapeutic effect of glucocorticoids combined with anticoagulants on the incidence of thrombotic complications among severely ill COVID-19 patients during the second wave, mortality was reduced, but thrombotic complication rates remained high and comparable to the first wave [3]. These studies stress the need for research on the mechanisms underlying thrombosis associated with COVID-19. Animals commonly used to study thrombosis pathophysiology (*i.e.* rats and mice) are naturally not susceptible to SARS-CoV-2 infection. Ferrets (*Mustela putorius furo*) are susceptible to SARS-CoV-2 infection and have been successfully used to study SARS-CoV-2 transmission [4–6]. In addition, ferrets have previously been used to study activation of coagulation and unravelled an influenza-induced pro-coagulant and prothrombotic state [7]. Here we studied COVID-19-associated changes in coagulation and thrombosis in lung material and plasma from SARS-CoV-2-inoculated ferrets that were part of a recent study on intranasal fusion inhibitory lipopeptides in preventing direct-contact SARS-CoV-2 transmission [8]. The materials were derived from ferrets assigned as donors in these transmission studies, and were directly inoculated intranasally with SARS-CoV-2 in a dose that efficiently and reproducibly transmitted SARS-CoV-2 to acceptor ferrets [8]. During the 20-day post inoculation monitoring these donor ferrets feature any clinical symptoms (*i.e.* no significant weight loss, changes in behaviour, posture, or signs of discomfort) and their clinical status should be classified as mild [8]. Lung material and plasma from these SARS-CoV-2-inoculated donor ferrets were analysed for COVID-19-associated changes in coagulation and thrombosis using histology and mass spectrometry (MS)-based proteomics. The latter approach allows for the simultaneous identification and quantification of hundreds of plasma proteins, including hemostatic and inflammatory signatures in human [9], and was now used for ferrets, a species for which very limited protein (immuno) assays are available. In addition, in contrast to activity- and immune-proteins assays, MS-based proteomics may be successfully used also for (ferret)plasma that has been subjected to a heat-inactivation step necessary to abolish infectivity of the potentially hazardous plasma.

2. Material and methods

2.1. Animal experiments

No animal experiments were performed specifically for the purpose of this study, all samples were collected in the framework of previous animal studies. Plasma and lung samples were collected from Influenza virus, SARS-CoV-2 and Aleutian Disease Virus seronegative young adult male (approximately 1 year old, weighing 1000-1500 g) ferrets (*M. putorius furo*) that were obtained from a commercial breeder (Triple F Farms, PA, USA), and were part of a recent study on intranasal fusion inhibitory lipopeptides in preventing direct-contact SARS-CoV-2 transmission [8]. Materials were derived from ferrets assigned as donors in these transmission studies, and were directly inoculated intranasally with 450 μl 5.4×10^5 TCID50/ml SARS-CoV-2 (isolate BetaCoV/Munich/BavPat1/2020) 225 μ per nostril, *i.e.* a dose that efficiently and reproducibly transmitted SARS-CoV-2 to mock-treated acceptor ferrets, for experimental details, see [8]). Up to 20 days after inoculation (DPI), at indicated time points (Fig. 1A), ferrets were weighed, swabs were collected from throat and nose for detection of SARS-CoV-2 genomes (viral load) using RT-qPCR [8,10]. Caval vein citrated (0.32%) blood (2 ml) was collected, centrifuged (2500 rpm, 15 min), and plasma was used for detection of SARS-CoV-2-specific antibodies using a virus neutralization (VN) endpoint titration assay [8] and stored at −80 °C. At 20 DPI, ferrets were euthanized and right lung lobules were dissected and stored in 10% formalin. Negative control plasma and lung materials were obtained from an unrelated study, from ferrets (*n* = 3) that were inoculated with measles virus. In these ferrets, measles virus proved replication-deficient (infectious virus could not be detected at any timepoint post-inoculation and infection did not result in clinical symptoms. These

samples were considered uninfected controls in this study [manuscript in preparation]. Additionally, we included EDTA-plasma (before (day −1) and up to 17 DPI) from ferrets (*n* = 3) that were inoculated with canine distemper virus (CDV) in a previously executed study, as positive controls [manuscript in preparation]. CDV-inoculated ferrets develop fatal disease with clear lung pathology [11]. All animal experiments were performed at Biosafety Level 3 (BSL3), and in compliance with national and institutional legislation on animal experimentation.

2.2. Lung histology

The right formalin-fixed lung lobules were sliced transversally into 9–10 segments of 5 mm, paraffin-embedded, and 5 μm-sections were stained with hematoxylin and eosin (HE). Serial sections were immuno-stained with an anti-(human) fibrinogen-γ goat polyclonal IgG antibody (0.4 mg/ml, sc-18,032, Santa Cruz Biotechnology) that binds ferret fibrinogen and fibrin (fibrin[ogen]). A normal goat IgG (IgGlAB-108-C, R&D systems) served as isotype control. Binding of primary antibodies was detected using rabbit polyclonal antibody to goat IgG conjugated to horseradish peroxidase (4 μg/ml, #GR89980–2, ABCAM), and visualized using diaminobenzidine (DAKO). HE- and immuno-stained sections were microscopically analysed by a European certified animal pathologist.

2.3. Plasma sample preparation for mass spectrometry

To permit plasma protein analysis outside BSL3 facilities, −80 °C stored and potentially hazardous plasma from virus infected ferrets was heat-inactivated (HI) at 56 °C for 1 h and centrifuged 10 min at 2500 rpm. This necessary HI-step precluded common plasma coagulation analysis (such as prothrombin time, activated partial thromboplastin time, and coagulation factor activity measurements). Therefore, and also as limited number of assays are available for ferret plasma (coagulations) proteins, we used a MS-based profiling technique that may allow quantifying many (ferret) plasma proteins simultaneously, despite the protein denaturing step preceding. After the HI-step, 10 μg HI-plasma protein was denatured, reduced and alkylated using 10 μl 1% Zwittergent 3–12 (Sigma-Aldrich, Germany), 10 mM Tris(2-choloroethyl) phosphate (ThermoFisher, USA) and 40 mM Chloroacetamide (Sigma-Aldrich, Germany). Proteins were digested overnight at 20 °C using 250 ng MS-grade trypsin (Promega). Peptides were purified using C18 cartridges on the AssayMAP Bravo platform (Agilent technologies) according to the manufacturer's protocol. The eluate was dried using a SpeedVac (Eppendorf), resuspended in 12 μl 2% *v/v* acetonitrile, 0.1% v/v trifluoroacetic acid. Tryptic peptides were analysed with Orbitrap Fusion (human samples) or Orbitrap Fusion Lumos Tribrid (ferret samples) mass spectrometer (ThermoFisher) *via* a nano electrospray ion source (ThermoFisher). Acquisition was previously described [12] for Orbitrap Fusion, with the exception of precursor scan window of 300 to 1600 *m/z* and ion count of 4×10^5. The Orbitrap Fusion Lumos Tribrid method was comparable, with following modifications. Buffer A was composed of 0.1% formic acid, buffer B of 0.1% formic acid, 80% acetonitrile. Peptides were loaded for 17 min at 300 nl/min at 5% buffer B, equilibrated for 5 min at 5% buffer B (17–22 min) and eluted by increasing buffer B from 5 to 27.5% (22–122 min) and 27.5–40% (122–132 min), followed by a 5-min wash to 95% and a 5 min regeneration to 5%. Survey scans of peptide precursors from 375 to 1500 *m/z* were performed at 120 K resolution (at 200 *m/z*) with a 4.0×10^5 ion count target. MS/MS was performed with the quadrupole with isolation window 0.7, HCD fragmentation with normalized collision energy of 30%, and rapid scans in the ion trap. The MS^2 ion count target was set to 3.0×10^4 and the max injection time was 20 ms. Only precursors with charge states 2–4 were sampled for MS^2. The dynamic exclusion was set to 30s.
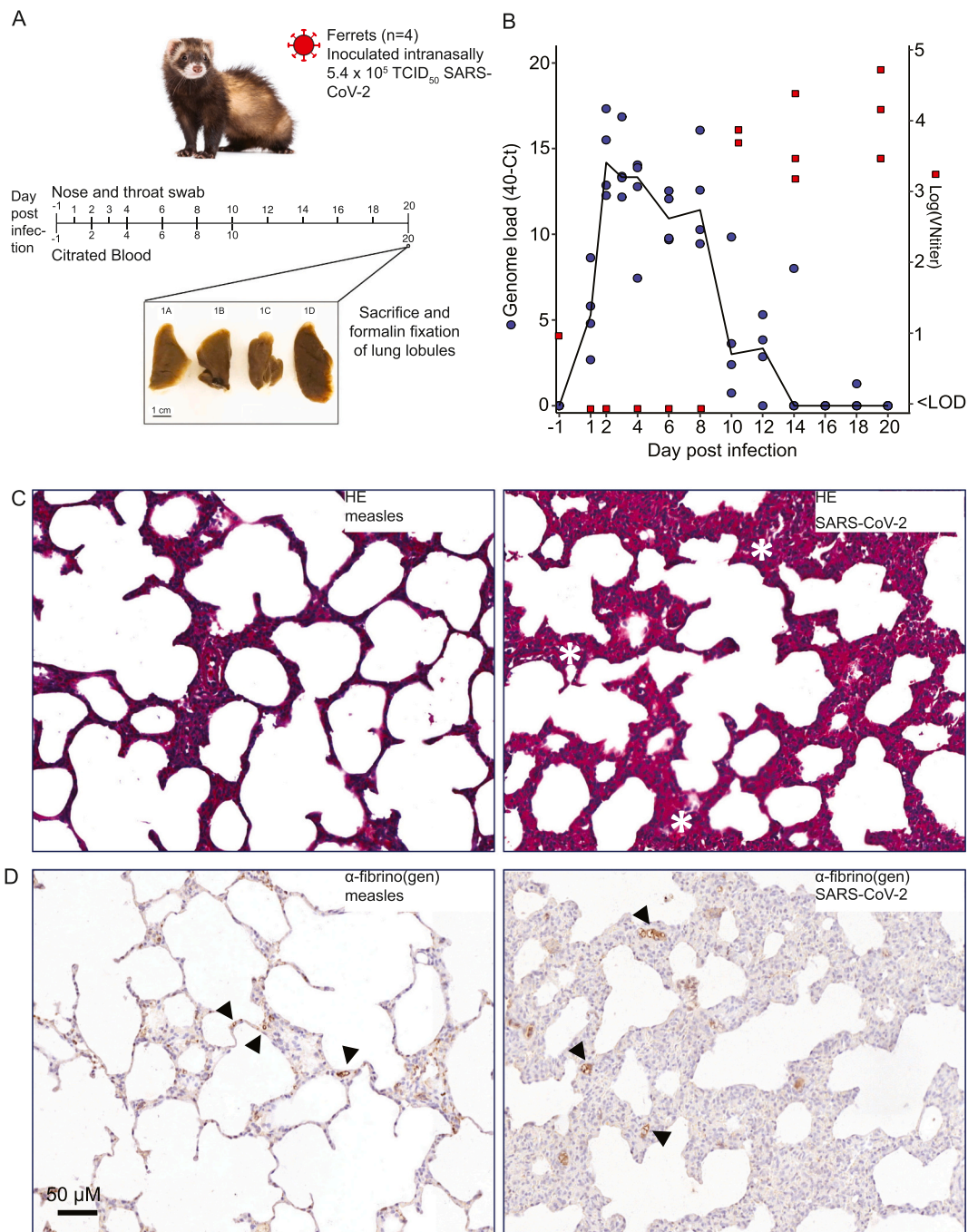
Fig. 1. Virus replication and lung histology after SARS-CoV-2 inoculation of ferrets. (A) Ferrets ($n = 4$) were inoculated intranasally with 5.4×10^5 median Tissue Culture Infectious Dose (TCID)50/ml of SARS-CoV-2. At the indicated days post inoculation (DPI) nose and throat swabs were taken for the detection of SARS-CoV-2 genomes. In addition, at the days indicated, citrated blood samples were taken for plasma proteomic profiling and detection of virus neutralizing antibodies. At 20 DPI the ferrets were sacrificed and the right lung lobules were processed for histological and immunohistochemical analysis. Ferret image Healthy Pets, Healthy People: Ferrets. [Internet]. (B) Virus genomes in throat swabs (blue circles) was determined by RT-qPCR. When the cycle threshold (Ct) was not surpassed after 40 cycles, the genome load was considered to be zero. Viral genomes detected in nose swabs showed comparable kinetics (not shown). Due to overlap in the datapoint not all are visible, values are below <LOD = limit of detection. Presence of virus neutralizing antibodies was determined (red squares), end-point serum dilution factor that block SARS-CoV-2 infection *in vitro* are displayed (VNtiter). (C) Images of representative hematoxylin and eosin staining of a 5 μm thick paraffin lung section obtained from a negative control ferret (left) and a SARS-CoV-2 inoculated ferret (right). Visible (left) is the honeycomb pattern of the alveoli and optical empty spaces typical for well-functioning lungs). Alveolar septa of SARS-CoV-2-inoculated ferrets were mildly expanded (right, white asterisks), mostly by macrophages, fewer lymphocytes, and showing an diffuse interstitial histiocytic pneumonia (not visible for the magnification presented here). (D) Fibrin(ogen) staining of slides serial to the HE slides presented in panel C. Black arrow heads; small positive spots from capillary vessels likely containing fibrinogen rather than pathological fibrin-rich microthrombi. Black bars represent 50 μm. Note: Screening on the specificity of the polyclonal anti-human fibrin(ogen) antibody used showed that this specifically bound to ferret fibrin(ogen), since no antibody-binding was observed in the IgG isotype controls (see methods, data not shown). (For interpretation of the references to colour in this figure legend, the reader is referred to the web version of this article.)

2.4. Data analysis

The RAW MS files were acquired with XCalibur software (Thermo-Fisher) and processed using MaxQuant 1.6.2.10 [13]. Peptides were searched against the *M. putorius furo* (June 2021) or homo sapiens (February 2019) Uniprot database using standard settings with the additional options match between runs. Output files were loaded in R 4.0.3. Proteins were filtered by "reverse" and "only identified by side" and LFQ-intensities were $\log_2$ transformed. Statistical significance was determined using the limma-package [14]. RAW files and search/identification files have been deposited in the PRIDE repository [15], PXD027582.

3. Result and discussion

3.1. SARS-CoV-2 productively infects ferrets

SARS-CoV-2 viral genomes were detected in throat (Fig. 1 B) and nose swabs (not shown) from all SARS-CoV-2 inoculated animals up to 10 days post inoculation (DPI.) From 8 DPI onwards, a strong decrease in SARS-CoV-2 genomes in the throat and nose was observed that coincided with the appearance of virus neutralizing (VN) antibodies in plasma from 10 DPI onwards (Fig. 1B). During the 20-day post inoculation monitoring ferrets did not show any clinical symptoms (*i.e.* no significant weight loss, changes in behaviour, posture, or signs of discomfort). Thus, the phenotype of SARS-CoV-2 inoculated ferrets should be classified as a mild phenotype.

3.2. Histopathology

Lung tissue of measles virus-inoculated ferrets (included as negative control) displayed normal histology on HE-stained sections (Fig. 1C). Alveolar septa of SARS-CoV-2-inoculated ferrets were mildly expanded by macrophages, fewer lymphocytes, showing a diffuse interstitial histiocytic pneumonia (Fig. 1C). Capillaries were engorged with red blood cells (capillary congestion, not shown). Red blood cells, did not feature compressed morphology that would have been indicative for active obstruction as in thrombosis (note, lungs were not perfused prior to harvesting). Moreover, epithelial hyperplasia, hyaline membranes, and mild pulmonary oedema were observed (not shown). Importantly, none of the HE-sections obtained from the SARS-CoV-2 inoculated ferrets provided evidence for the presence of fibrin deposition and/or (microvascular) thrombosis.

As the fibrin-specific monoclonal antibody 59D8 [16] did not cross-react with ferret fibrin (not shown), a goat anti-human fibrinogen-γ polyclonal antibody was used for detection of fibrin (thrombosis). This antibody binds both ferret fibrinogen and fibrin (fibrin(ogen)) and allows discrimination of these solely by means of morphological appearance and localisation. Fibrin(ogen)was observed in the (larger) blood vessels of all three-measles virus inoculated (control) ferrets (not shown), as well as the smaller capillaries (Fig. 1D). The absence of apparent pathology in these healthy control lungs suggests that this most likely represented trapped post-mortem plasma fibrinogen and fibrin rather than antemortem formed fibrin (thrombosis). There was no further evidence for the presence of fibrinogen/fibrin-rich structures in measles control lung tissue. Fibrin(ogen) immunostaining of lungs from SARS-CoV-2-inoculated ferrets was confined to multifocal antibody-positive spots in the alveolar walls, which was observed in all four ferrets (Fig. 1 D). Likely these small spots were from capillary vessels containing fibrinogen rather than pathological fibrin-rich microthrombi, since comparable structures were also observed in the measles control sections (Fig. 1D). Thus, the lung tissue from SARS-CoV-2-inoculated ferrets (at 20 DPI) showed several features of interstitial inflammation however, there was no evidence of (microvascular) thrombosis.

3.3. MS-based plasma proteomics

To detect changes in the plasma proteome in SARS-CoV-2-inoculated ferrets, we used a plasma proteomics profiling approach that has successfully been used for the analysis of human plasma [9]. This allows simultaneous identification and quantification of hundreds of plasma proteins, including hemostatic and inflammatory signatures. Since plasma samples of SARS-CoV-2-inoculated ferrets were heat inactivated (HI) prior to export from BSL3, we assessed the effect of HI on the plasma proteome of healthy human individuals ($n = 3$). HI had a minor impact on the human plasma proteome, with the exception of fibrinogen (FGA, FGG, FGB), ficolin3 and carboxypeptidase N catalytic chain 1 (Fig. 2A). In agreement with these observations, also for ferret plasma ($n = 1$), the relative abundance of plasma proteins measured was not affected by HI (Fig. 2B). Thus, in both human and ferret plasma we observed that the majority of the plasma proteome was not affected by HI, apart from fibrinogen. We hypothesize that fibrinogen may be particularly susceptible to protein precipitation induced by HI, thereby affecting the reproducibility and accuracy of protein quantification. Although all plasmas were subjected to identical sample handling, which should control for the impact of the heat-inactivation step, care should be taken in reviewing the results obtained for these proteins, in particular fibrinogen and ficolin-3. We next used the MS-based proteomics-approach to analyse HI-plasmas collected longitudinally from CDV-inoculated animals (from a previously executed study, included as positive controls, see methods section) and SARS-CoV-2-inoculated animals. Despite the fact that the FASTA file for *M. putorius furo* has not extensively been reviewed and curated we were able to quantify 323 proteins, including 24 proteins that are marked as coagulation-related [17].

Statistical analysis revealed that CDV inoculation of ferrets had a larger effect on the plasma proteome than SARS-CoV-2 inoculation (Fig. 2C). In total 40 proteins were significantly altered from 6 DPI onwards for CDV (Fig. 2D), including IgM, CD5-ligand, S100A9, and CD14, all known to have a role in an (innate) immune response. Moreover, an increase in acute phase proteins (*i.e.* serum amyloid A, ferritin, haptoglobin and hemopexin) was observed. This confirms the presence of both an inflammatory and innate immune response following CDV, which is in line with the observed clinical signs and histopathological changes, including lymphopenia, fever, weight loss and marked pathology leading to fatal disease [11]. Thus, the MS-based plasma proteomics approach allowed for profiling of ferret plasma in disease (*i.e.* CDV) and we proceeded with exploring the impact of SARS-CoV-2 on the ferret plasma protein profile.

In contrast to marked differences in plasma protein abundance in CDV-inoculated ferrets, SARS-CoV-2 inoculation resulted in limited differences in plasma protein levels. In total 10 proteins were significantly altered over time, including serum amyloid A, ceruloplasmin, and haptoglobin (Fig. 2E). These proteins are well-known to respond in the acute phase following (virus) infections. Additionally, after an initial decrease between 4 and 6 DPI, an overall increase of lipase A and apolipoprotein B and C3 was observed over time. Those proteins are involved in lipid metabolism, suggesting that alteration may possibly reflect on ferret metabolism to cope with the increased demand of lipids, which are needed for virus replication [18]. With the exception of FGG, no other coagulation factors were changed as the majority of which demonstrated a low coefficient of variation (Fig. 2F). The small changes in abundance of FGG should be carefully reviewed in light of the effects of heat inactivation on fibrinogen plasma levels. Therefore, it is difficult to make a clear statement about the abundance of FGG in SARS-CoV-2 inoculated ferrets.

4. Conclusion

To the best of our knowledge, this is the first report of plasma proteomics on ferrets, an experimental animal model frequently used to
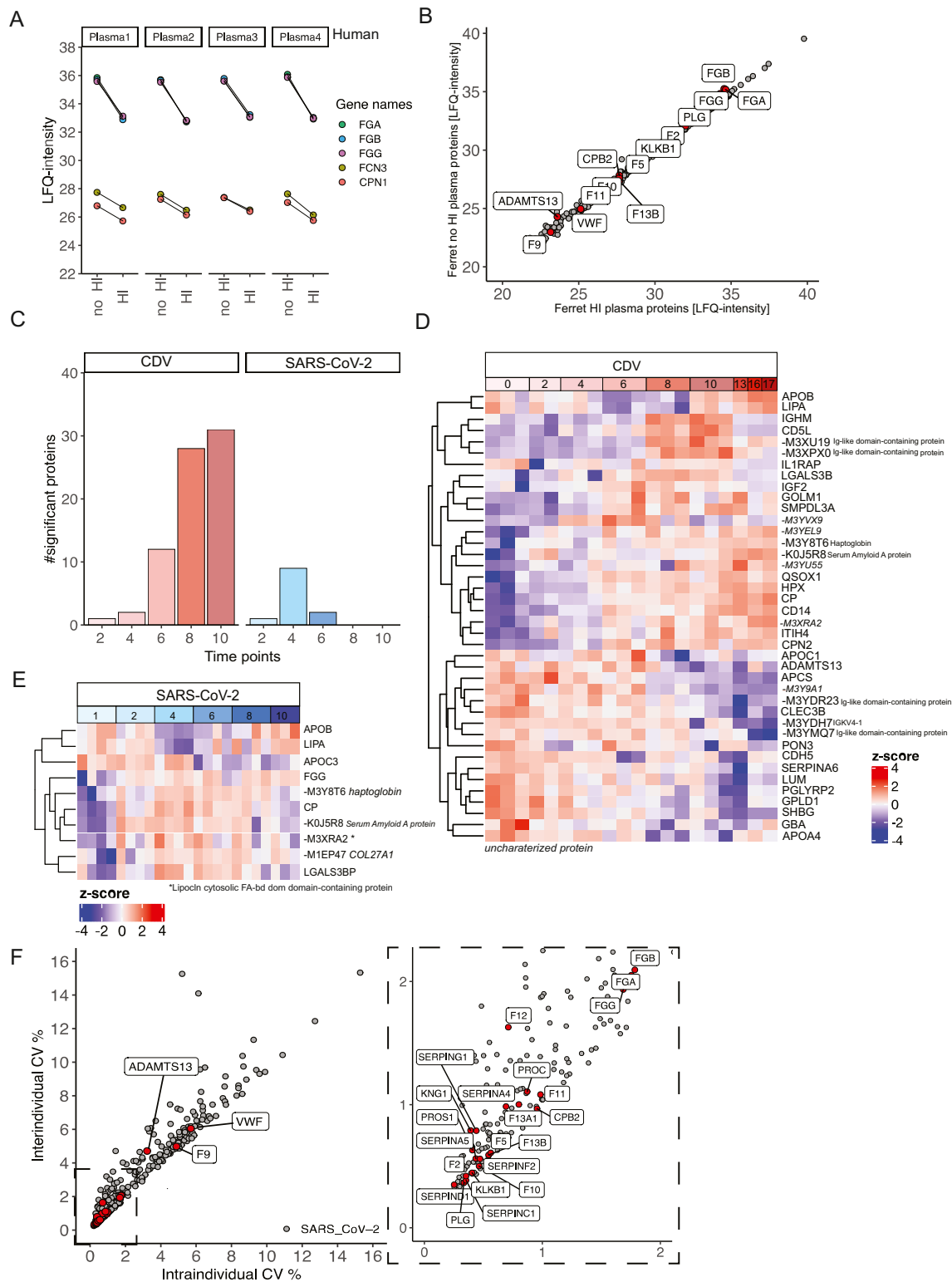
Fig. 2. Plasma profiling mass spectrometry approach on ferrets with CDV- and SARS-CoV-2-inoculated ferrets. (A) Label-free Mass-spectrometry analysis shows impact of heat-inactivation on healthy individual (human) citrated plasma samples by decreased levels of fibrinogens (FGA, FGG, FGB), ficolin3 (FCN3) and carboxypeptidase N catalytic chain 1 (CPN1). (HI: heat inactivation plasma, no-HI: non heat inactivated plasma) (B) Direct comparison of heat-inactivated and non-heat-inactivated citrated ferret plasma depicts the limited impact of heat inactivation on the ferret plasma proteome. (C) Number of significantly altered proteins between day 0 and 10 for CDV- and SARS-CoV-2-inoculated ferrets (D) Hierarchical clustering of z-scored median LFQ-intensities for 40 significant proteins following over time for inoculation with CDV. (E) Hierarchical clustering of z-scored median LFQ intensities for significant 10 proteins over time following SARS-CoV-2 inoculation. Including serum amyloid A (SAA), haptoglobin (HP), ceruloplasmin (CP), fibrinogen gamma (FGG), apolipoprotein B (APOB), lipase A (LIPA), lipocalin (LCN). (F) The inter-individual and intra-individual variation of protein levels calculated as the means coefficient of variation (CV) for each protein within each SARS-CoV-2-inoculated ferret and across all analysed SARS-CoV-2-inoculated ferrets. Zoom-in highlights coagulation proteins within a CV of 2%.

study viral infections. Plasma profiling shows the ability to detect plasma protein alterations in a severe disease phenotype, as shown for canine distemper virus (CDV)-inoculated ferrets. Although the ferret model has proven useful to study the transmission of SARS-CoV-2, the present study using materials collected in the framework of previous studies, indicates that ferrets are of limited use to understand the impact of severe COVID-19 on human lung tissue and COVID-19-associated thrombosis [8]. This corresponds to the observation that ferrets only display a mild disease phenotype with limited involvement of the lower respiratory tract, in the absence of clear lung pathology. An experimental animal susceptible to SARS-CoV-2 and less able to deal with the viral challenge, such as hamsters [19] or human angiotensin-converting enzyme-2 transgenic mice [20–22], may be more suited to study changes relevant to COVID-19-associated coagulation and thrombosis. Such a model is essential as thrombo-(embolic) complications are still a major contributor to morbidity and mortality in COVID-19.

Authorship contributions

RDdV, MPMdM, MvdB, BJMvV designed the study. MPMdM, MvdB, BJMvV, RLdS, AM, MP acquired funding. KSS and RDdV performed the animal experiment and carried out plasma and tissue collection. CvdZ and ICK performed proteomics experiments. ICK and AJH performed data analysis. RRAW and FT performed the histology and were microscopically analysed with DCFS. ICK, RRAW, FJT, CvdZ, KSS, AJH, DCFS, RDdV, MPMdM, MvdB, BJMvV interpreted the data. RRAW, FJT, ICK, MvdB and BJMvV drafted the manuscript. ICK, DCFS, RDdV, MPMdM, MvdB, BJMvV revised the manuscript. All authors reviewed the manuscript and approved the final version.

Disclosures

None.

Declaration of Competing Interest

None.

Acknowledgement

References

[1] F.A. Klok, Kruip MJHA, Vandermeer NJM, M.S. Arbous, Gommers DAMPJ, K. M. Kant, Incidence of thrombotic complications in critically ill ICU patients with COVID-19, in: Thrombosis Research [Internet] 191, Elsevier, 2020, pp. 145–147, https://doi.org/10.1016/j.thromres.2020.04.013. Available from: doi:.

[2] S.S. Hasan, S. Radford, C.S. Kow, S.T.R. Zaidi, Venous thromboembolism in critically ill COVID-19 patients receiving prophylactic or therapeutic anticoagulation: a systematic review and meta-analysis, J. Thromb. Thrombolysis 50 (2020) 814–821.

[3] D.C. Coalition, Kaptein FHJ, Stals MAM, M. Grootenboers, E. Braken, Burggraaf JLI, Incidence of thrombotic complications and overall survival in hospitalized patients with COVID-19 in the second and first wave, Thromb. Res. 199 (2021) 143–148.

[4] M. Richard, A. Kok, D. de Meulder, T.M. Bestebroer, M.M. Lamers, N.M.A. Okba, SARS-CoV-2 is transmitted via contact and via the air between ferrets, in: Nature Communications [Internet] 11, Springer US, 2020, pp. 1–6, https://doi.org/10.1038/s41467-020-17367-2. Available from: doi:.

[5] J.S. Kutter, D. de Meulder, T.M. Bestebroer, P. Lexmond, A. Mulders, M. Richard, SARS-CoV and SARS-CoV-2 are transmitted through the air between ferrets over more than one meter distance, in: Nature Communications [Internet], Springer US, 2021, p. 12, https://doi.org/10.1038/s41467-021-21918-6. Available from: doi:.

[6] S.G. Kim, S.M. Kim, E.H. Kim, S.J. Park, K.M. Yu, Kim Yil, Infection and rapid transmission of SARS-CoV-2 in ferrets, in: Cell Host and Microbe [Internet] 27, Elsevier Inc, 2020, pp. 704–709, https://doi.org/10.1016/j.chom.2020.03.023, e2. Available from:.

[7] M. Goeijenbier, E.C.M. van Gorp, J.M.A. van den Brand, K. Stittelaar, K. Bakhtiari, J.J.T.H. Roelofs, et al., Activation of coagulation and tissue fibrin deposition in experimental influenza in ferrets, BMC Microbiol. 14 (2014).

[8] R.D. de Vries, K.S. Schmitz, F.T. Bovier, C. Predella, J. Khao, D. Noack, et al., Intranasal fusion inhibitory lipopeptide prevents direct-contact SARS-CoV-2 transmission in ferrets, Science 1382 (2021) 1379–1382.

[9] P.E. Geyer, N.A. Kulak, G. Pichler, L.M. Holdt, D. Teupser, M. Mann, in: Plasma Proteome Profiling to Assess Human Health and Disease. Cell Systems [Internet] 2, Elsevier Ltd, 2016, pp. 185–195, https://doi.org/10.1016/j.cels.2016.02.015. Available from:.

[10] V.M. Corman, O. Landt, M. Kaiser, R. Molenkamp, A. Meijer, Chu DKW, Detection of 2019 novel coronavirus (2019-nCoV) by real-time RT-PCR, in: Eurosurveillance [Internet], European Centre for Disease Prevention and Control (ECDC), 2020, p. 25, https://doi.org/10.2807/1560-7917.ES.2020.25.3.2000045. Available from:.

[11] R.D. de Vries, M. Ludlow, A. de Jong, L.J. Rennick, R.J. Verburgh, G. van Amerongen, et al., Delineating morbillivirus entry, dissemination and airborne transmission by studying in vivo competition of multicolor canine distemper viruses in ferrets, PLoS Pathog. 13 (2017) 1–22.

[12] E. Stokhuijzen, J.M. Koornneef, B. Nota, B.L. van den Eshof, F.P.J. van Alphen, M. van den Biggelaar, et al., Differences between platelets derived from neonatal cord blood and adult peripheral blood assessed by mass spectrometry, J. Proteome Res. 16 (2017) 3567–3575.

[13] N. Neuhauser, A. Michalski, R.A. Scheltema, M. Mann, J.V. Olsen, in: Andromeda : A Peptide Search Engine Integrated into the MaxQuant Environment, 2011, pp. 1794–1805.

[14] B. Phipson, S. Lee, I.J. Majewski, W.S. Alexander, G. Smyth, Robust hyperparameter estimation protects, Ann. Appl. Stat. 10 (2016) 946–963.

[15] E.W. Deutsch, A. Csordas, Z. Sun, A. Jarnuczak, Y. Perez-Riverol, T. Ternent, The ProteomeXchange consortium in 2017: supporting the cultural change in proteomics public data deposition, Nucleic Acids Res. 45 (2017), D1100–6.

[16] M. Heestermans, S. Salloum-asfar, D. Salvatori, E.H. Laghmani, B.M. Luken, S. Zeerleder, et al., Role of platelets, neutrophils, and factor XII in spontaneous venous thrombosis in mice, Blood 127 (2018) 2630–2637.

[17] KEGG Pathway: Compelement and Coagulation Cascades- Homo Sapiens (2021) [Internet], Available from:, 2021 Jun 29 //www.genome.jp/kegg-bin/show_path way?hsa04610.

[18] M. Abu-Farha, T.A. Thanaraj, M.G. Qaddoumi, A. Hashem, J. Abubaker, F. Al-Mulla, The role of lipid metabolism in COVID-19 virus infection and as a drug target, Int. J. Mol. Sci. 21 (2020).

[19] J.F. Chan, A.J. Zhang, S. Yuan, V.K. Poon, C.C. Chan, A.C. Lee, W.M. Chan, Z. Fan, H.W. Tsoi, L. Wen, R. Liang, J. Cao, Y. Chen, K. Tang, C. Luo, J.P. Cai, K.H. Kok, H. Chu, K.H. Chan, S. Sridhar, Z. Chen, Chen, K.K. To, K.Y. Yuen, Simulation of the clinical and pathological manifestations of coronavirus disease 2019 (COVID-19) in a golden syrian hamster model: implications for disease pathogenesis and transmissibility, Clin. Infect. Dis. 71 (9) (2020) 2428–2446, https://doi.org/10.1093/cid/ciaa325.

[20] C. Lee, A.C. Lowen, Animal models for SARS-CoV-2, Curr. Opin. Virol. (2021) 48.

[21] P.B. McCray, L. Pewe, C. Wohlford-Lenane, M. Hickey, L. Manzel, L. Shi, et al., Lethal infection of K18- hACE2 mice infected with severe acute respiratory syndrome coronavirus, J. Virol. 81 (2007) 813–821.

[22] L. Bao, W. Deng, B. Huang, H. Gao, J. Liu, L. Ren, et al., The pathogenicity of SARS-CoV-2 in hACE2 transgenic mice, Nature 583 (2020) 830–833.